Available online at www.eccomasproceedia.org
Eccomas Proceedia SMART (2023) 140-149

ECCOMAS
Proceedia

X ECCOMAS Thematic Conference on Smart Structures and Materials
SMART 2023
D.A. Saravanos, A. Benjeddou, N. Chrysochoidis and T. Theodosiou (Eds)

STRATEGIES FOR REDUCING OPERATIONAL AMPLIFIER OUTPUTS IN PIEZOELECTRIC SHUNT WITH NEGATIVE CAPACITANCE

M. BERARDENGO*, S. MANZONI, O. THOMAS†, C. GIRAUD-AUDINE† AND M. VANALI††**

*Department of Mechanical, Energy, Management and Transportation Engineering
Università degli Studi di Genova
Genoa, Italy
e-mail: marta.berardengo@unige.it

** Department of Mechanical Engineering
Politecnico di Milano
Milan, Italy
e-mail: stefano.manzoni@polimi.it

†Ecole Nationale Supérieure d'Arts et Métiers
Arts et Métiers Sciences et Technologies
Lille, France
e-mail: Olivier.THOMAS@ensam.eu, christophe.giraud-audine@ensam.eu

††Department of Engineering and Architecture
Università degli Studi di Parma
Parma, Italy
e-mail: marcello.vanali@unipr.it

Abstract. The use of piezoelectric shunt is an attracting approach for vibration attenuation since it allows avoiding the use of feedback sensors and digital/analog controllers by exploiting the special features of piezoelectric elements. Indeed, in piezoelectric shunt, the piezoelectric element acts at the same time as sensor and actuator and the control action is tuned by a proper electric impedance through which the piezoelectric element is shunted. Once the position of the piezoelectric element on the structure to be controlled, as well as its features, and the shunt impedance are optimized, the maximum achievable control performance is fixed. An approach to further improve the attenuation is to insert a negative capacitance (NC) in the shunt impedance, making it semi-active since NCs are realized by means of operational amplifier-based circuits. Although the NC is able to significantly increase the attenuation by artificially enhancing the modal electro-mechanical coupling factor, it poses some issues due to its active nature. One of the most important, and seldom treated in the literature, is that, when the external forcing increases, the outputs (particularly, the output voltage) of the operational amplifier can saturate, leading to an non-proper functioning of the control system.

Peer-review under responsibility of the organizing committee of SMART 2023.
doi: 10.7712/150123.9772.444339

This paper analyses at first how to decrease the operational amplifier outputs by keeping the attenuation performance unaltered. This is achieved by properly tuning the values of some specific resistances of the NC circuit, which will be shown to be able to regulate the amplifier outputs without affecting the control performance. Then, the paper addresses the problem of finding a balance between control performance and extent of the outputs in cases where the previous setting of the mentioned resistances is not able to prevent saturation. Since different circuits exist for building NCs, the previous analyses will be carried out for different circuit layouts to compare them in terms of risk of saturation of the operational amplifier.

Key words: piezoelectric shunt, resistive shunt, negative capacitance, operational amplifier, saturation, vibration, damping

1 INTRODUCTION

The use of piezoelectric shunt is a widely used approach for reducing vibrations (e.g., [1, 2, 3, 4, 5]). It consists in connecting a proper impedance (shunt impedance) to the terminals of a piezoelectric element [6, 7, 8], particularly, a piezoelectric-bender is considered here. This requires to optimise the features of the piezoelectric element as well as its position on the vibrating structure. Such an optimisation allows increasing as much as possible the Modal Electro-Mechanical Coupling Factor (MEMCF), which is a measure of the energy conversion in the coupled system.

Once the MEMCF is optimised the performance achievable with the control system is maximised. To further improve it, one of the main ways is to add a Negative Capacitance (NC) in the shunt circuit because this element is able to artificially increase the MEMCF value to a new Enhanced Modal Electro-Mechanical Coupling Factor (EMEMCF). NCs do not exist in nature but can be simulated by using circuits based on an Operational Amplifier (OP-AMP). There are two main issues related to the use of NCs: (i) dynamical instability can arise because of the active nature of OP-AMPs and (ii) saturation of the OP-AMP output can occur in case the excitation to the system increases and this leads to a non-proper functioning of the shunt circuit with a consequent worsening of the control action. While the former problem has been already addressed in different works (e.g., [9, 10, 11]) giving stability thresholds on the NC value, the latter has not been deeply treated in the literature.

This paper aims at first at investigating how it is possible to decrease the OP-AMP output without changing the attenuation performance and, then, at evidencing how OP-AMP outputs and attenuation performance are linked. To do this, the special case of resistive shunt enhanced by an NC is considered (i.e., the shunt impedance is constituted by an NC and a resistance R) because resistive shunt with an NC allows for broadband attenuation ([12, 13]) and its control performance is significant. Therefore, this shunt configuration offers many advantages compared to, e.g., resonant shunt [13]. Although the paper treats the specific case of a piezoelectric patch, the discussion and the theory on which the analyses are based can be easily extended to stacks. However, this case deserves further in-depth analyses since problems could be faced,

due to the possible large current involved and the different capacitance value which characterizes the piezoelectric stacks.

The paper is structured as follows: Section 2 gives the bases about the system model used and the NC configurations considered here, Section 3 shows how to change the OP-AMP output without changing the attenuation performance, and Section 4 discusses the link between OP-AMP outputs and attenuation. Finally, Section 5 presents an experimental campaign to validate the theoretical outcomes.

2 SYSTEM MODEL AND NC CONFIGURATIONS

This section firstly introduces the model used to describe the dynamics of the coupled system in Section 2.1 and, then, the way to connect the NC to the piezoelectric element in Section 2.2.

2.1 The model of the coupled system

A generic structure is excited by a force F and a piezoelectric actuator bonded to the structure is shunted with an electric impedance Z_{sh}. V is the voltage between the piezoelectric electrodes, while Q is the charge in one electrode ($-Q$ in the other electrode). The displacement W of a generic point x of the structure at time t can be expressed by means of a modal summation [14], thus exploiting the modal coordinates q_i, being i = 1, . . . , N and N the number of modes, and the eigenmodes ϕ_i scaled to the unit modal mass and with the piezoelectric patch short-circuited. The modal coordinates are the solutions of the problem:

$$\ddot{q}_i + 2\xi_i\omega_i\dot{q}_i + \omega_i^2 q_i - \chi_i V = F_i, \quad \forall i = 1, ..., N \tag{1}$$

$$C_\infty V - Q + \sum_{i=1}^{N} \chi_i q_i = 0 \tag{2}$$

Here, ω_i is the i-th eigenfrequency of the coupled system with the piezoelectric element short-circuited, ξ_i is the associated non-dimensional damping ratio and F_i is the modal force. Furthermore, C_∞ is the electrical capacitance of the piezoelectric patch with blocked structure, which also corresponds to the value of the capacitance at infinite frequency [10]. χ_i is the i-th modal coupling coefficient. Equation (1) is the equations of motion of the system and χ_i couples these N equations of motion to Eq. (2) that models the system electric behaviour. Moreover, $\ddot{q}_i$ and $\dot{q}_i$ are the second and first derivative of q_i with respect to t, respectively. It is finally remarked that V and $\dot{Q}$ (i.e. the derivative of Q with respect to t, which is a current) are linked by Z_{sh} (Fig. 1) and, thus, such a link is a function of on the type of shunt impedance layout. This link constitutes a further equation in addition to Eqs. (1) and (2).

A single-degree-of-freedom (SDOF) approximation can be performed in case of low modal superimposition. In this case, for $\Omega \simeq \omega_i$ (where Ω is the angular frequency), Eq. (1) is written only for the i-th mode and Eq. (2) becomes:

$$C_{\mathrm{p},i} V - Q + \chi_i q_i = 0 \tag{3}$$

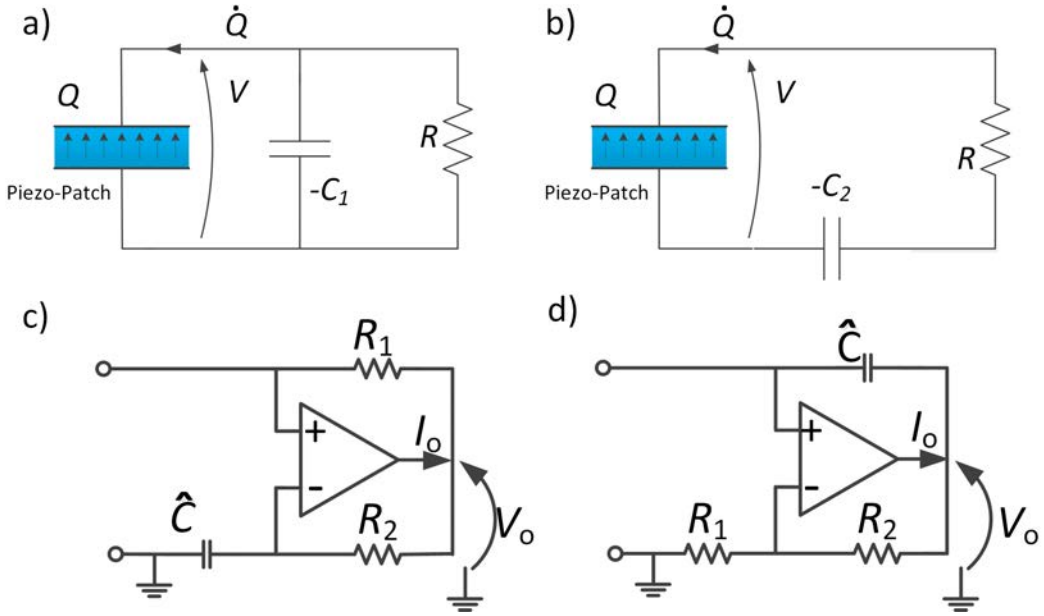

Figure 1: Parallel (a) and series (b) connection of the NC, and type A (c) and type B (d) layouts for building the NC. The schematics of plots (c) and (d) are valid for NCs in parallel. When NCs in series are considered the OP-AMP pins must be exchanged.

where $C_{\mathrm{p},i}$, referred to as modal capacitance, can be found by measuring the value of the capacitance of the piezoelectric actuator midway between ω_i and ω_{i+1}. More details about $C_{\mathrm{p},i}$ and its estimation are available in [15, 16].

It is also noticed that, for each mode, the MEMCF k_i can be derived from Eqs. (1) and (3):

$$k_i = \frac{\chi_i}{\omega_i \sqrt{C_{\mathrm{p}i}}}, \quad |k_i| \simeq \sqrt{\frac{\hat{\omega}_i^2 - \omega_i^2}{\omega_i^2}} \tag{4}$$

where $\hat{\omega}_i$ the i-th eigenfrequency of the system with the piezoelectric element open-circuited.

2.2 NC connections and layouts

When Z_{sh} is made from an NC and a resistance R, two layouts can be used for the electric connection: parallel and series (see Fig. 1a and b. Here, $-C_1$ denotes the NC in the parallel layout, while $-C_2$ indicates the NC in the series layout). The series layout is usually used to mitigate low-order modes, while the parallel connection is employed to control high-order modes [10].

Each NC can be built using two different layouts: A (Fig. 1c) and B (Fig. 1d). Both generates an NC equal to $\hat{C}R_2/R_1$. For series NC, other more complicated layout can be used in practice to solve different electrical problems (e.g., [17]). However, they can be traced back to the layouts already presented in Figs. 1c and d (see [10] for more details).

3 THE REDUCTION OF OP-AMP OUTPUTS WITHOUT REDUCING THE ATTENUATION PERFORMANCE

According to Eqs. (1) and (2) and the schematics of Figs. 1a and b, the amplitudes M of the frequency response functions G between the charge Q_{cs} (where $Q_{\mathrm{cs}} = \sum_{i=1}^{N} \chi_i q_i$ for the model considering all the modes and $Q_{\mathrm{cs}} = \chi_i q_i$ for the SDOF model), produced by the deflection of the piezoelectric element due to structural vibrations, and the OP-AMP outputs (i.e., current I_0 and voltage V_0; see Figs. 1c and d) are:

$$M^{\mathrm{v}}_{\mathrm{pa}} = |G^{\mathrm{v}}_{\mathrm{pa}}| = |\frac{V_{0,\mathrm{pa}}}{Q_{\mathrm{cs}}}| = \frac{\sqrt{1 + (\Omega C_1 R_1)^2}}{P}, \quad M^{\mathrm{i}}_{\mathrm{pa}} = |G^{\mathrm{i}}_{\mathrm{pa}}| = |\frac{I_{0,\mathrm{pa}}}{Q_{\mathrm{cs}}}| = \frac{\Omega C_1 [1 + (R_1/R_2)]}{P} \tag{5}$$

$$M^{\mathrm{v}}_{\mathrm{pb}} = |G^{\mathrm{v}}_{\mathrm{pb}}| = |\frac{V_{0,\mathrm{pb}}}{Q_{\mathrm{cs}}}| = \frac{1 + (R_2/R_1)}{P}, \quad M^{\mathrm{i}}_{\mathrm{pb}} = |G^{\mathrm{i}}_{\mathrm{pb}}| = |\frac{I_{0,\mathrm{pb}}}{Q_{\mathrm{cs}}}| = \frac{\sqrt{(\Omega C_1)^2 + (1/R_1)^2}}{P} \tag{6}$$

$$M^{\mathrm{v}}_{\mathrm{sa}} = |G^{\mathrm{v}}_{\mathrm{sa}}| = |\frac{V_{0,\mathrm{sa}}}{Q_{\mathrm{cs}}}| = \frac{\sqrt{1 + (\Omega C_2 R_1)^2}}{S}, \quad M^{\mathrm{i}}_{\mathrm{sa}} = |G^{\mathrm{i}}_{\mathrm{sa}}| = |\frac{I_{0,\mathrm{sa}}}{Q_{\mathrm{cs}}}| = \frac{\Omega C_2 [1 + (R_1/R_2)]}{S} \tag{7}$$

$$M^{\mathrm{v}}_{\mathrm{sb}} = |G^{\mathrm{v}}_{\mathrm{sb}}| = |\frac{V_{0,\mathrm{sb}}}{Q_{\mathrm{cs}}}| = \frac{1 + (R_2/R_1)}{S}, \quad M^{\mathrm{i}}_{\mathrm{sb}} = |G^{\mathrm{i}}_{\mathrm{sb}}| = |\frac{I_{0,\mathrm{sb}}}{Q_{\mathrm{cs}}}| = \frac{\sqrt{(\Omega C_2)^2 + (1/R_1)^2}}{S} \tag{8}$$

The subscripts "pa", "pb", "sa" and "sb" indicate the type of NC connection (i.e., p for parallel, and s for series) and NC layout (i.e., A and B). Furthermore:

$$P = \sqrt{(C_1 - C_\infty)^2 + 1/(\Omega R)^2}, \quad S = \sqrt{(C_2 - C_\infty)^2 + (\Omega R C_2 C_\infty)^2} \tag{9}$$

More details about the way to obtain all these expressions can be found in [18].

Equations (5) to (8) are dependent on parameters influencing the attenuation (i.e., R and either C_1 or C_2), which are not changed because the first analysis proposed here attempts to study how to reduce the OP-AMP outputs without affecting the control performance. However, it is noticed that all these equations are also function of a parameter (i.e., either R_1 or the ratio between R_1 and R_2) which can be changed without affecting the attenuation performance. Therefore, studying the trends of M as function of these parameters, the following conclusions can be achieved:

- R_1 must be increased to decrease $M^{\mathrm{i}}_{\mathrm{b}}$, and decreased to decrease $M^{\mathrm{v}}_{\mathrm{a}}$;
- R_1/R_2 must be increased to decrease $M^{\mathrm{v}}_{\mathrm{b}}$, and decreased to decrease $M^{\mathrm{i}}_{\mathrm{a}}$.

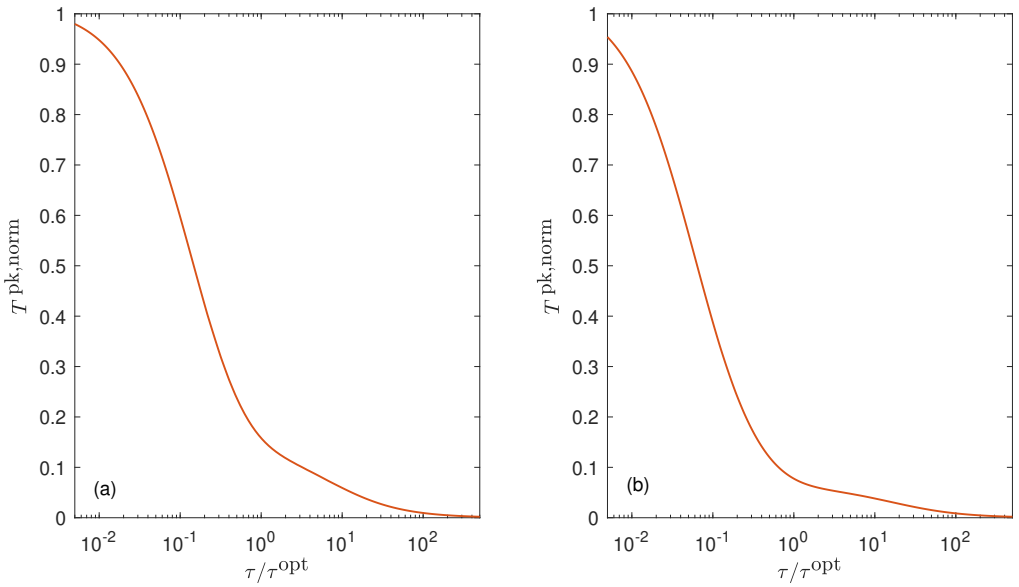

Figure 2: Trend of T^{pk} for OP-AMP output voltage with NC in series (Type A) for two different systems: $|k_i|$=0.1 and C_2=(10/3)$C_{\mathrm{p},i}$ (a) and $|k_i|$=0.1 and C_2=(10/7)$C_{\mathrm{p},i}$ (b). All the curves are normalized (as indicated by the superscript 'norm') in order to have 1 as the maximum value in each plot for a straightforward comparison of the trends. ξ_i=10^{-3}, $\omega_i/(2\pi)$=30 Hz, $C_{\mathrm{p},i}$=30 nF, R_1=6 kΩ (R_1/R_2 has no effect here).

The effects of these increase/decrease of the parameters R_1 and R_1/R_2 sometimes are equal at all frequencies, while are frequency-dependent in some other cases (see Eqs. (5) to (8)). More detailed analyses are available in [18].

4 THE REDUCTION OF OP-AMP OUTPUTS CHANGING THE ATTENUATION PERFORMANCE

In this section, the values of R and either C_1 or C_2 (depending on the considered connection type) are changed to check the effect on the OP-AMP outputs. To do this, the SDOF system is considered because it allows an easier comprehension of the results without any loss of generality, Using the variables k_i, $\tilde{k}_i$ (i.e., the EMEMCF [10]) and τ ($\tau = RC_{\mathrm{eq}}$, where C_{eq} is an equivalent capacitance depending on the NC value and $C_{\mathrm{p},i}$ [10]), the expressions of the frequency response functions G for the i-th mode become [18]:

$$G^{\mathrm{v}}_{i,\mathrm{pa}} = \frac{V_{0,\mathrm{pa}}}{Q_{\mathrm{cs}}} = \frac{\tilde{k}_i^2 + \mathrm{j}\Omega C_{\mathrm{p},i}(\tilde{k}_i^2 - k_i^2)R_1}{P_i\tilde{k}_i^2}, \quad G^{\mathrm{i}}_{i,\mathrm{pa}} = \frac{I_{0,\mathrm{pa}}}{Q_{\mathrm{cs}}} = \frac{\mathrm{j}\Omega C_{\mathrm{p},i}(\tilde{k}_i^2 - k_i^2)(1 + (R_1/R_2))}{P_i\tilde{k}_i^2} \tag{10}$$

$$G^{\mathrm{v}}_{i,\mathrm{pb}} = \frac{V_{0,\mathrm{pb}}}{Q_{\mathrm{cs}}} = \frac{1 + (R_2/R_1)}{P_i}, \quad G^{\mathrm{i}}_{i,\mathrm{pb}} = \frac{I_{0,\mathrm{pb}}}{Q_{\mathrm{cs}}} = \frac{\mathrm{j}\Omega C_{\mathrm{p},i}(\tilde{k}_i^2 - k_i^2) + \tilde{k}_i^2/R_1}{P_i\tilde{k}_i^2} \tag{11}$$

$$G^{\mathrm{v}}_{i,\mathrm{sa}} = \frac{V_{0,\mathrm{sa}}}{Q_{\mathrm{cs}}} = \frac{(\tilde{k}_i^2 - k_i^2) + \mathrm{j}\Omega C_{\mathrm{p},i}\tilde{k}_i^2 R_1}{S_i(\tilde{k}_i^2 - k_i^2)}, \quad G^{\mathrm{i}}_{i,\mathrm{sa}} = \frac{I_{0,\mathrm{sa}}}{Q_{\mathrm{cs}}} = \frac{\mathrm{j}\Omega C_{\mathrm{p},i}\tilde{k}_i^2[1 + (R_1/R_2)]}{S_i(\tilde{k}_i^2 - k_i^2)} \tag{12}$$

$$G^{\mathrm{v}}_{i,\mathrm{sb}} = \frac{V_{0,\mathrm{sb}}}{Q_{\mathrm{cs}}} = \frac{1 + (R_2/R_1)}{S_i}, \quad G^{\mathrm{i}}_{i,\mathrm{sb}} = \frac{I_{0,\mathrm{sb}}}{Q_{\mathrm{cs}}} = \frac{\mathrm{j}\Omega C_{\mathrm{p},i}\tilde{k}_i^2 + (\tilde{k}_i^2 - k_i^2)/R_1}{S_i(\tilde{k}_i^2 - k_i^2)} \tag{13}$$

where:

$$P_i = -C_{\mathrm{p},i}\frac{(1 + \mathrm{j}\Omega\tau)k_i^2}{\mathrm{j}\Omega\tau\tilde{k}_i^2}, \quad S_i = C_{\mathrm{p},i}(1 + \mathrm{j}\Omega\tau)\frac{k_i^2}{(\tilde{k}_i^2 - k_i^2)} \tag{14}$$

Since the frequency response function between the modal force F_i and the modal coordinate q_i is [10]:

$$H_i = \frac{1 + \mathrm{j}\Omega\tau}{(\omega_{i,\mathrm{sc}}^2)^2 - (1 + 2\xi_i\omega_i\tau)\Omega^2 + \mathrm{j}\Omega[\tau\omega_{i,\mathrm{oc}}^2 + 2xi_i\omega_i - \tau\Omega^2]} \tag{15}$$

the frequency response function T_i between F_i and either V_0 or I_0 can be found as:

$$T_i^{\mathrm{v}} = \chi_i\phi_i(x_{\mathrm{f}})G_i^{\mathrm{v}}H_i, \quad T_i^{\mathrm{i}} = \chi_i\phi_i(x_{\mathrm{f}})G_i^{\mathrm{i}}H_i \tag{16}$$

where x_{f} is the point where the external force is applied, $\omega_{i,\mathrm{sc}}$ is the eigenfrequency when R is null in Figs. 1a and b, and $\omega_{i,\mathrm{oc}}$ is the eigenfrequency when R is infinite in Figs. 1a and b.

If the amplitudes of the frequency response functions T_i^{v} and T_i^{i} are considered, it is possible to notice that their peaks are at frequency values corresponding to (or very close to) the peak value of the amplitude of the frequency response function H_i. Figure 2 shows, for two electro-mechanical systems chosen as examples, the trend of the peaks of T_i^{v}, named T^{pk}, as functions of the value of τ (the value of τ is expressed in the figure as normalised over its optimal value τ^{opt}, i.e., the value which maximises the vibration attenuation for the mode considered [10]) for a type A NC in series. The value of τ is changed on the horizontal axis of the plot by changing the value of the shunt resistance R, keeping always the same value for the NC and, thus, for the C_{eq} involved in the definition of τ [10]. The figure shows that the value of T^{pk} is small when $\tau \geq \tau^{\mathrm{opt}}$, while it increase when $\tau < \tau^{\mathrm{opt}}$. Similar results are obtained for type B NCs in series, and also for the corresponding current output. Therefore, for NCs in series, all the modes higher than that for which τ is optimised generate a small requirement on OP-AMP outputs because they are characterised by an optimal value of τ smaller than that used, while lower modes (which require higher values of τ for an optimal tuning [10]) produce large outputs. Since series NCs are used for controlling low-order modes [10], this feature is advantageous. For NCs in parallel, the plot of Fig. 2 is almost horizontally mirrored around τ/τ^{opt}=1. Since NCs in parallel are usually used to attenuate high-order modes, this is again advantageous. In general, it is possible to conclude that OP-AMP outputs are reduced in series NCs increasing R, and in parallel NCs decreasing R. As for the value of the NC, the closer the NC is to $C_{\mathrm{p},i}$, the larger the OP-AMP outputs are. More detailed analyses can be found in [18].

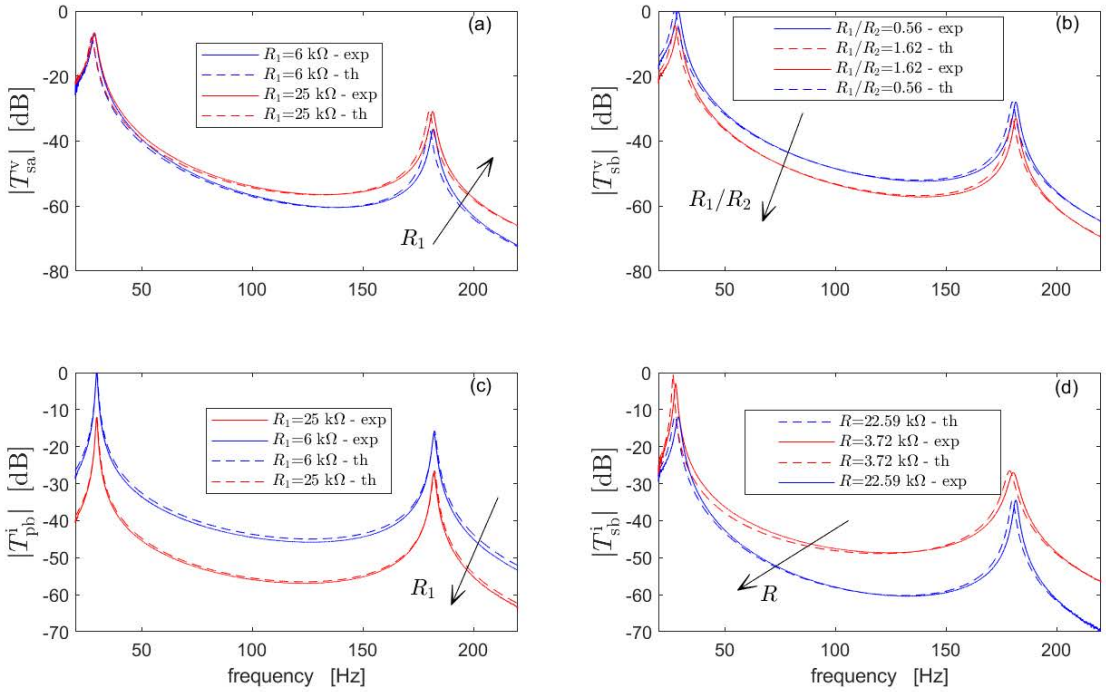

Figure 3: Amplitudes of T for different tests. In each plot the NC and R values are kept equal for all the curves, exception made for the R value in plot (d).

5 EXPERIMENTS

The experiments carried out to validate the previous theoretical outcomes have been performed relying on a cantilever beam equipped with two piezoelectric patches electrically connected in series and bonded to the beam at the clamped end on opposite sides. The vibration response was measured with a contact-less laser velocimeter and the excitement was provided with a properly designed electro-magnetic device [19]. The first two eigenfrequencies associated to bending modes are at about 29 and 181 Hz.

Figures 3a to c show that the values of R_1 and R_1/R_2 are able to change the OP-AMP outputs according to the bulleted list in Section 3. For all the tests in this figure the attenuation performance did not change because the NC and R values were kept constant. Furthermore, Fig. 3d shows, as an example, that an increase of the R value for an NC in series leads to a decrease of the OP-AMP voltage output, in accordance to the analysis of Section 4. It is noticed that all the theoretical curves in Fig. 3 have been obtained using a multi-modal model presented in [18], which is based on the analysis presented here. More details and test results can be found in [18].

6 Conclusion

This paper has addressed the problem of reducing the OP-AMP outputs when using NCs in resistive piezoelectric shunt for vibration control. The paper has shown that it is possible to reduce the outputs without affecting the control performance. Furthermore, the effect on OP-AMP outputs of the parameters involved in the vibration reduction has been evidenced. The theoretical results have been validated by means of an experimental campaign.

REFERENCES

[1] B. Zhou, F. Thouverez, and D. Lenoir, "Vibration reduction of mistuned bladed disks by passive piezoelectric shunt damping techniques," *AIAA Journal*, vol. 52, no. 6, pp. 1194–1206, 2014.

[2] J. F. Toftekær, A. Benjeddou, J. Høgsberg, and S. Krenk, "Optimal piezoelectric resistive-inductive shunt damping of plates with residual mode correction," *Journal of Intelligent Material Systems and Structures*, vol. 29, no. 16, pp. 3346–3370, 2018.

[3] F. Xie, Y. Su, W. Zhou, and W.-Z. Zhang, "Design and evaluation of a shunted flexible piezoelectric damper for vibration control of cable structures," *Smart Materials and Structures*, vol. 28, no. 8, p. article ID. 085031, 2019.

[4] L. Pernod, B. Lossouarn, J.-A. Astolfi, and J.-F. Deü, "Vibration damping of marine lifting surfaces with resonant piezoelectric shunts," *Journal of Sound and Vibration*, vol. 496, 2021.

[5] G. Raze, J. Dietrich, B. Lossouarn, and G. Kerschen, "Shunts vs networks: tuning and comparison of centralized and decentralized piezoelectric vibration absorbers," *Smart Materials and Structures*, vol. 31, no. 11, 2022.

[6] P. Soltani, G. Kerschen, G. Tondreau, and A. Deraemaeker, "Tuning of a piezoelectric vibration absorber attached to a damped structure," *Journal of Intelligent Material Systems and Structures*, vol. 28, no. 9, pp. 1115–1129, 2017.

[7] B. Lossouarn, L. Rouleau, R. Darleux, and J.-F. Deü, "Comparison of passive damping treatments based on constrained viscoelastic layers and multi-resonant piezoelectric networks," *Journal of Structural Dynamics*, no. 1, pp. 30–48, 2021.

[8] G. Konda Rodrigues, P. Gardonio, L. Dal Bo, and E. Turco, "Piezoelectric patch vibration control unit connected to a self-tuning rl-shunt set to maximise electric power absorption," *Journal of Sound and Vibration*, vol. 536, p. 117154, 2022.

[9] B. de Marneffe and A. Preumont, "Vibration damping with negative capacitance shunts: theory and experiment," *Smart Materials And Structures*, vol. 17, no. 3, p. Article ID 035015, 2008.

[10] M. Berardengo, O. Thomas, C. Giraud-Audine, and S. Manzoni, "Improved resistive shunt by means of negative capacitance: new circuit, performances and multi mode control," *Smart Materials and Structures*, vol. 25, p. Article ID 075033, 2016.

[11] M. Berardengo, S. Manzoni, O. Thomas, and M. Vanali, "Guidelines for the layout and tuning of piezoelectric resonant shunt with negative capacitances in terms of dynamic compliance, mobility and accelerance," *Journal of Intelligent Material Systems and Structures*, vol. 32, no. 17, pp. 2092–2107, 2021.

[12] S. Behrens, A. J. Fleming, and S. O. R. Moheimani, "A broadband controller for shunt piezoelectric damping of structural vibration," *Smart Materials and Structures*, vol. 12, no. 1, pp. 18–28, 2003.

[13] M. Berardengo, S. Manzoni, M. Vanali, and R. Bonsignori, "Enhancement of the broadband vibration attenuation of a resistive piezoelectric shunt," *Journal of Intelligent Material Systems and Structures*, vol. 32, no. 18-19, pp. 2174–2189, 2021.

[14] O. Thomas, J. Ducarne, and J. De$\ddot{u}$, "Performance of piezoelectric shunts for vibration reduction," *Smart Materials and Structures*, vol. 21, no. 1, p. 015008, 2012.

[15] M. Berardengo, S. Manzoni, J. Høgsberg, and M. Vanali, "Vibration control with piezoelectric elements: The indirect measurement of the modal capacitance and coupling factor," *Mechanical Systems and Signal Processing*, vol. 151, p. 107350, 2021.

[16] M. Berardengo, S. Manzoni, O. Thomas, and M. Vanali, "Piezoelectric resonant shunt enhancement by negative capacitances: optimisation, performance and resonance cancellation," *Journal of Intelligent Material Systems and Structures*, vol. 29, no. 12, pp. 2581–2606, 2018.

[17] S. Moheimani and A. Fleming, *Piezoelectric Transducers for Vibration Control and Damping*. Springer-Verlag, 2006.

[18] M. Berardengo, S. Manzoni, O. Thomas, C. Giraud-Audine, L. Drago, S. Marelli, and M. Vanali, "The reduction of operational amplifier electrical outputs to improve piezoelectric shunts with negative capacitance," *Journal of Sound and Vibration*, vol. 506, p. 116163, 2021.

[19] O. Thomas, C. Touz$\acute{e}$, and A. Chaigne, "Asymmetric non-linear forced vibrations of free-edge circular plates. part ii: experiments," *Journal of Sound and Vibration*, vol. 265, no. 5, pp. 1075–1101, 2003.